Available online at www.sciencedirect.com
SCIENCE DIRECT®

Journal of the European Ceramic Society 24 (2004) 3437–3445

www.elsevier.com/locate/jeurceramsoc

Grain growth anisotropy of β-silicon nitride in rare-earth doped oxynitride glasses

R.L. Satet*, M.J. Hoffmann

Institute for Ceramics in Mechanical Engineering, University of Karlsruhe (TH), Haid-und-neu-strasse 7, D-76131 Karlsruhe, Germany

Abstract

Grain growth experiments in oversaturated Me–Si–Mg–O–N glasses were carried out for six different metallic elements (Me = Sc, Lu, Yb, Y, Sm and La). These elements all form a cation with a +3 valence but have increasing ionic radius. Ostwald ripening was observed for all compositions and showed that anisotropy of growth increases with increasing Me^{3+} radius. Cyclic heat treatments of the samples revealed furthermore that growth anisotropy is controlled by the adsorption behaviour of the cation at the interface between grain and intergranular film. The use of elements of the same valence (Sc, Y) but different electronic structures than the rare-earth elements (Lu, Yb, Sm and La) showed that the electronic structure has a major role on the adsorption behaviour of the Me^{3+} cation.

Keywords: Glass; Grain growth; Interfaces; Oxynitride glass; Rare-earth oxide; Si_3N_4

1. Introduction

The main reason for the outstanding mechanical properties of silicon nitride is related to the formation of a so-called in-situ reinforced microstructure upon phase transformation and densification.[1–7] Best toughness is achieved when a bimodal distribution of grain size exists and the large grains are elongated with an aspect ratio over 4. It has been showed that the composition of the sintering additives have a significant influence on microstructure development. Sanders and Mieskowski[8] found for rare-earth doped silicon nitrides with RE = Y, Ce, Sm or La the largest grains in the Y-based composition. Goto and Thomas[9] reported largest grains when Yb or Dy are used. Pyzik and Beaman[10] reported microstructure variations when MgO, CaO and Y_2O_3 content changed, from coarse in MgO doped ceramics, to bimodal in samples doped with Y_2O_3 and CaO, to fine monomodal if simultaneously MgO, CaO and Y_2O_3 were used. Though, there exist only few quantitative data and simulations on grain growth of silicon nitride, and to our knowledge only one systematic investigation of the impact of rare-earth sintering additives.[11] Most grain growth models reported in the literature refer to the Ostwald ripening theory, where grain growth as a function of time is described by

$$\left(d^n - d_0^n\right) = K \cdot t \tag{1}$$

with d_0 the mean grain size at $t = 0$, d the mean grain size at each time t and K a constant. If the rate limiting step is the attachment reaction at the surface, n take the value 2 and if it take the value 3, growth is controlled by diffusion. Measurements were made on loose powders or seeded materials and reveal fluctuations for n between 3 and 5. The main reason for divergence of the results from the theoretically predicted growth exponents might be that the major conditions for applying the Lifshitz–Slyozow–Wagner (LSW) theory,[12,13] i.e. a dilute system and isotropic growth, are not fulfilled in the case of the silicon nitride ceramic. Models exist that made some attempts to the description of anisotropic Ostwald ripening. Bernard-Granger et al.[14] presented a modified equation of Eq. (1) that takes into account different exponents and activation energies for growth in length and in diameter. They showed exponents of 3 for the length and 5 for the diameter growth and an abrupt change in the activation energies at 1780 °C, but did not explain it. Kitayama et al.[15] investigated grain growth of loose silicon nitride powder sintered with SiO_2 and Y_2O_3 at different temperatures. Their simulations[16] are in good agreement with the experimental results they present, and predict again growth exponents

* Corresponding author.
E-mail addresses: raphaelle.satet@ikm.uni-karlsruhe.de (R.L. Satet), mjh@ikm.uni-karlsruhe.de (M.J. Hoffmann).

0955-2219/$ - see front matter © 2003 Elsevier Ltd. All rights reserved.
doi:10.1016/j.jeurceramsoc.2003.10.034

of 3 for attachment controlled and 5 for diffusion controlled growth. Still, the volume fraction condition of the LSW-theory they used is again not fulfilled for these loose powders, and the diffusion fields of the particles influence each other. Therefore oversaturated oxynitride glasses were designed[17] in which a low volume fraction of Si_3N_4 grains is dispersed in a glass matrix. In this case, the diffusion fields of the particles do not interact and Ostwald ripening can be assumed. Further advantage of these experiments is that, on the contrary of the ceramic, no steric hindrance[18] takes place.

The equilibrium shape of silicon nitride in vacuum has been calculated by Kraemer et al.[19] using the Periodic-Bond-Chain theory. The atomic structure of the prominent faces revealed to be partly responsible for the anisotropic grain growth in silicon nitride. The atomic roughness of the basal planes, observed for grains dispersed in an oxynitride glass, allow a diffusion controlled growth whereas the prism planes are atomically smooth so that the rate limiting step for their growth is the attachment reaction. Since the equilibrium shape is a function of the surface energy, it necessarily changes with the composition of the surrounding material. In silicon nitride ceramics, grains are separated by a continuous amorphous film, that results from the sintering additives needed for liquid phase sintering. Rare-earth oxides or Y_2O_3 are commonly used sintering aids. They are necessary not only for easier sintering,[20,21] but also because they induce intergranular crack growth[22] and thus increased toughness. Therefore, it proved relevant to investigate grain growth anisotropy of β-Si_3N_4 in rare-earth based oxynitride glasses.

The rare-earth elements all form a cation with a $+3$ valence. It has been showed for glass compositions containing a rare-earth oxide and Al_2O_3 that the properties of the intergranular film, like composition and thickness, scales with the radius of the Me^{3+} cation.[23] The intergranular film that forms between two grains in the polycrystalline material also forms between flocculated particles in the glass. The film thickness, and therefore its composition, were showed to be equivalent in both the ceramic and the glass, provided the same elements were used. Therefore, one can assume that the reaction at the interface between grain and surrounding glass are the same in both the ceramic and the oversaturated glass and grain growth experiments on glasses with low volume fraction of free growing grains are a reliable model for grain growth in bulk ceramics. Moreover, thermo-mechanical properties of the rare-earth based oxynitride glasses, as bulk material, also proved to directly depend on the cation size of Me^{3+}.[24–27] In all studies,[23] a merely different behavior was found for the Y-based, compared to the rare-earth based compositions. Yttrium also forms a cation with $+3$ valence but does not belong to the rare-earth elements. The present study focussed on the glass compositions with six different Me^{3+} cations: Sc^{3+}, Lu^{3+}, Yb^{3+}, Y^{3+}, Sm^{3+}, La^{3+}. We will address the impact on grain growth of cation size and of different electronic configuration by comparing elements from the 3rd column of the periodic table with rare-earth elements. Moreover, existing investigations were all carried out on compositions containing Al_2O_3,[17,15] in which SiAlON formation that influence grain growth depends on the cation size. In this study we used, instead of Al_2O_3, MgO that does not form a solid solution with Si_3N_4, so that a more accurate description of the role of the cation size on grain growth anisotropy will arise.

2. Experimental procedures

In order to investigate the impact of the radius of different ions on grain growth six elements were chosen. They all form a cation with a $+3$ valence and are all considered to present a coordination number of six in oxynitride glasses. In Table 1 the corresponding cation sizes are listed. These six elements can be furthermore partitioned in two groups: Sc, Y and La belongs to the 3rd column of the periodic table of the elements, La, Sm, Yb and Lu are rare-earth elements. They show what is commonly known as the lanthanide contraction, so that the radius of their cation decreases with an increase in the atomic weight (Table 1).

Powder batches were prepared by weighing proper amounts of Si_3N_4 (SN-E10, UBE Industries, Japan), SiO_2 (Aerosil OX50, Degussa, Germany), MgO (MgO, UBE Industries, Japan) and a Me_2O_3 [La_2O_3 (Lanthan (III)-Oxid LAB, Merck, Germany], Lu_2O_3 (Lutetium Oxide, Meldform Rare Earth, United Kingdom), Sm_2O_3 (Samarium Oxide, Meldform Rare Earth, United Kingdom), Sc_2O_3 (Scandium Oxide, Meldform Rare Earth, United Kingdom), Y_2O_3 (Yttriumoxid feinst, H. C. Starck, Germany), Yb_2O_3 (Yb2O3 99.99, Shin-Etsu Chemical, Japan) in order to reach the compositions listed in Table 1. In a former paper, those compositions were showed to be oversaturated in nitrogen, so that the

Table 1
Glass compositions in eq.% as a function of Me contained in the glass

	Composition					Atomic weight (g)	Cation size[34] (Å)
	Me	Si	Mg	O	N		
Sc	20	60	20	22	78	44.96	0.73
Lu	20	60	20	22	78	147.973	0.85
Yb	20	60	20	22	78	173.04	0.86
Y	20	60	20	24	76	88.91	0.89
Sm	20	60	20	26	74	150.4	0.96
La	20	60	20	28	72	138.9	1.05

Cation size of Me^{3+} is given under the assumption of a coordination number of 6. Atomic weight is of Me.

solubility limit of Si_3N_4 is exceeded and Si_3N_4 grains remain in the glass after heat treatment. The powders were mixed in a planetary ball mill for 1 h at 300 rotations/min with Si_3N_4 grinding media in 2-propanol. The powders were subsequently dried and sieved. Green bodies of ~22 mm in diameter and ~10 mm high were first uniaxially pressed at 20 MPa and then cold isostatically pressed at 400 MPa. Each sample was placed in a BN crucible on a powder bed of an equimolar mixture of the sample powder and BN powder. The BN crucibles were then placed in a graphite crucible on a Si_3N_4:SiO_2 (1:1) powder bed, as sketched in Fig. 1. The samples were first melted at 1700 °C for 30 min under a nitrogen overpressure of 2.2 MPa. A maximum cooling rate of 25 °C/min was achieved by switching off the furnace. After this heat-treatment the samples have a droplet shape (Fig. 2), that indicates completed melting. Further annealing was carried out as a cyclic heat treatment at a temperature of 1600 °C for 2 h then 6 h and 10 h. Therefore, annealing states will be further referred to as 2, 8, and 18 h dwell-time.

After each annealing period, the samples were cut in two pieces, one of which was used for characterization, the other one for further annealing. The polished samples were plasma etched with a CF_4:O_2 Plasma[28] for characterization in an SEM. Length and diameter of the grains that present a rectangular shape were measured as defined in Fig. 3, and the aspect ratio was calculated for each grain. After each heat treatment between 50 and 150 grains were measured in each sample, in order to determine the distribution.

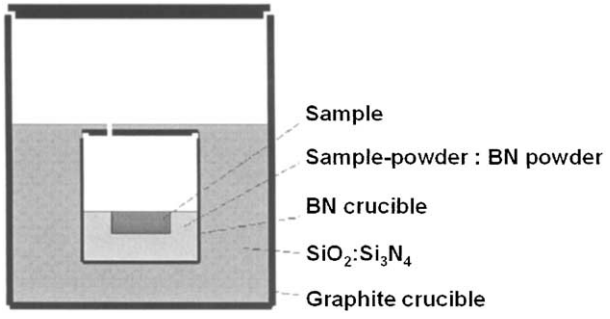

Fig. 1. Sample crucible arrangement for heat treatment in the gas pressure sintering furnace.

Fig. 2. Glass bead of the Lu-based glass after heat treatment at 1700 °C.

3. Results

The following section describes the variations in grain size and aspect ratio distribution with increasing annealing time as the radius of the Me^{3+} cation changes. The results are sustained by definition and measurements of a growth ratio, that depends on the composition of the oxynitride glass. It has to be preliminary stated, that the Si_3N_4 powder used for the preparation of the glasses consists up to 95% of the α-modification of the crystal. Therefore, during any heat treatment first a phase transformation occurs, where the driving force for grain dissolution or growth is much different than during a pure Ostwald ripening. It has been showed that grain growth anisotropy of Si_3N_4 changes dramatically between phase transformation and Ostwald ripening stage.[17] All grains dispersed in the oxynitride glasses after melting of the green body present either an hexagonal or a rectangular shape (Fig. 3). Silicon nitride grains of the α-phase would have a rounded shape. Therefore one can assume, that all α-Si_3N_4 grains have been dissolved, and that the α/β phase transformation is completed in all glass compositions after melting at 1700 °C. Grain growth in following cyclic annealing experiments can thus be considered as a unique Ostwald ripening mechanism.

3.1. Grain growth as a function of radius of Me^{3+}

The aspect ratio distribution as a function of the diameter of each grain is plotted in Fig. 4 for the Lu-based

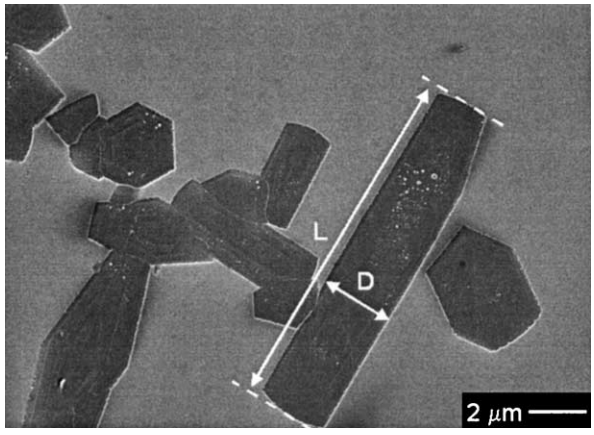

Fig. 3. Measurements of length (L) and diameter (D) of the Si_3N_4 grains on polished surfaces.

glass and in Fig. 5 for the La-based glass after either 2 or 18 h dwell-time at 1600 °C. The aspect ratio distribution after 2 h annealing at 1600 °C will be considered as the starting distribution. In the Lu-based glass, β-Si_3N_4 grains have aspect ratios between 2 and 12, whereas in the La-based glass aspect ratios of up to 20 are reached. Morphology of the silicon nitride grains in the La-based glass presents a higher anisotropy than in the Lu-based glass.

When annealing is increased to 18 h, the distributions of the aspect ratio as a function of the grain diameter flatten. At low diameters the aspect ratio of the grains is lower than after 2 h of annealing. This phenomenon is more pronounced in the Lu-based glass than in the La-based glass. In the Lu-based glass all grains present an aspect ratio between 1 and 5.5. In the La-based glass the grain size distribution is still very broad, with aspect ratios between 2 and 15.

In order to compare grain sizes in the different glass compositions, we consider the grains with the highest diameters in the distribution after the longest annealing, i.e. l8 h. These grains are, from the available data-sets, the grains with the nearest shape to an equilibrium shape. In Fig. 6, this near-equilibrium aspect ratio is plotted as a function of the radius of Me^{3+}, under the assumption that all ions present a six-fold coordination. The near-equilibrium aspect ratio of β-Si_3N_4 increases linearly with increasing radius of the Me^{3+} cation from 2 in the Lu-based glass to 7.5 in the La-based glass. Furthermore there are two distinct correlations depending on whether Me^{3+} belongs to the 3rd group of the periodic table of the elements or to the lanthanides. This is an experimental evidence that not only the cation size by itself but also the electronic structure of the Me^{3+} cation has an influence on grain growth.

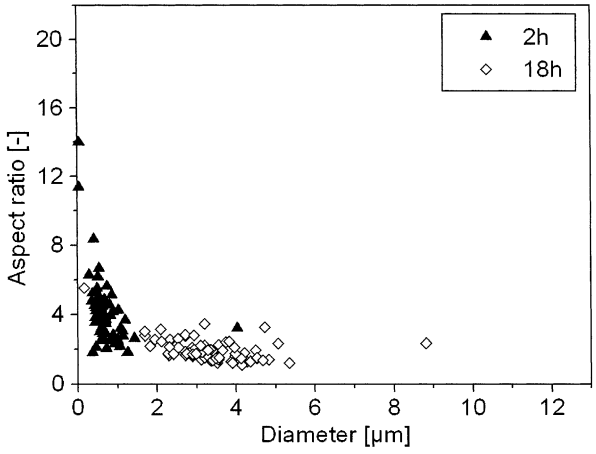

Fig. 4. Aspect ratio distribution as a function of diameter of grains in a Lu-based glass after 2 h or 18 h dwell time at 1600 °C.

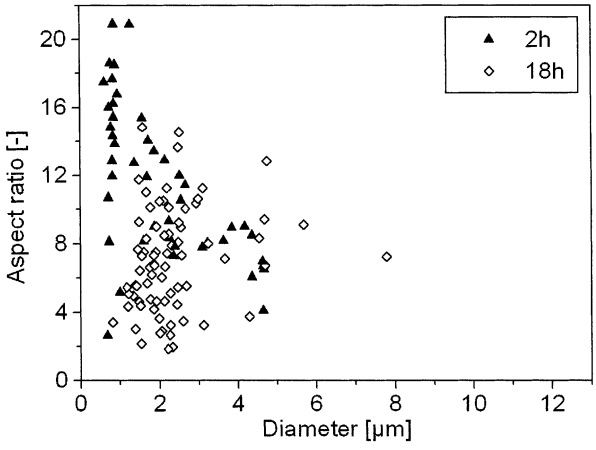

Fig. 5. Aspect ratio distribution as a function of diameter of grains in a La-based glass after 2 h or l8 h dwell time at 1600 °C.

3.2. Growth ratio

Plasma etched polished surfaces of the cyclic heat treated samples show in the Si_3N_4 grains deeper etched bands of roughly 100 nm in thickness (Fig. 7). These bands are equally thick in both [001] and [210] crystallographic directions. Such transient bands were also detected on grains dispersed in Al–RE–Si–O–N glasses and were showed to grow under diffusion controlled conditions during cooling, because of the high supersaturation.[29] Taking into account that these transient bands thus mark the end and the beginning of each annealing period, the exact net growth of the grain during each dwell-time at 1600 °C can be measured in both [001] and [210] directions.

We define the ratio of $\Delta l/\Delta d$ as growth ratio (Fig. 7). It describes the net growth in length Δl relatively to the net growth in diameter Δd and is therefore independent of both the absolute diameter of each grain and the dwell-time. The growth ratio as a function of the radius of Me^{3+} (Fig. 8) shows the same increasing correlation as the near-equilibrium aspect ratio (Fig. 6). It increases from 2 in the Lu-based glass to 10 in the La-based glass. Furthermore, it seems again that the value obtained in

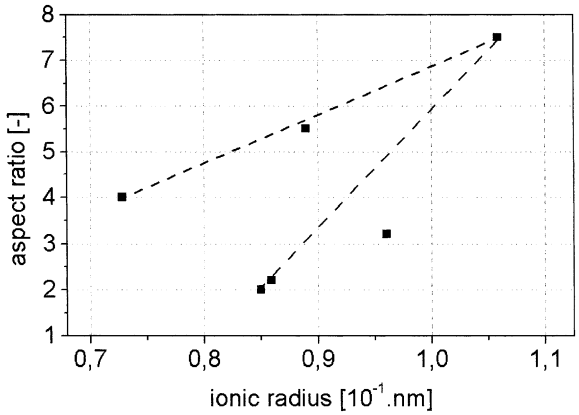

Fig. 6. Near-equilibrium aspect ratio as a function of the Me^{3+} cation radius.

the Y-based glass does not fit exactly in the correlation obtained for the lanthanides.

4. Discussion

4.1. Anisotropic Ostwald ripening

Kraemer described at the end of the α/β phase transformation, in a Y-based oxynitride glass containing Al, an aspect ratio–diameter distribution that decreases with increasing diameter of the grains and matches the distributions shown in Figs. 4 and 5 for the Lu- and La-based glasses. Although the reasons for the development of such a grain size distribution is not clear, the state assumed in this set of experiments as starting state correlates well with literature data from the end of the α/β phase transformation, and seems to form independently of the composition of the surrounding glass.

Aspect ratio–diameter distributions flatten with increasing annealing time. Existing analysis of the grain growth mechanism of silicon nitride are based on the resolution of flux equations considering that the driving force for mass transport is created by variation of the chemical potential between the (100) and the (001) planes.[16] As treated by Kraemer for Y–Si–Al–O–N glasses, grains grow preferentially in length[30] so that the solution of the flux equations is independent from the diameter.[31] Kitayama et al.[16] developed a flux equation controlled by both diffusion and interfacial reaction as rate limiting steps and took into account diameter as well as length growth. Both authors come to the same conclusions and experimental evidences, that grains with the smallest diameter in the distribution will dissolve. Because diameter≪length, dissolution occurs preferentially in length in order to minimize the differences between the chemical potentials between prism and basal planes. Since length decreases faster than the diameter the mean aspect ratio decreases and the distribution broadens at low diameters, and the overall distribution flattens. In this, it corresponds to part of the predicted Ostwald ripening mechanism. Though, Kitayama[15] also showed some measurements of increasing aspect ratio of the largest grains after a regime of constant aspect ratio independently of grain diameter. This was not observed in the present experiment. Possible explanations will be discussed in the following paragraph.

The kinetic evolution of the aspect ratio–diameter distributions is strongly dependent on the radius of Me^{3+}. In the Lu-based glass the distribution flattens much faster than in the La-based glass. Moreover the distribution for the La-based glass is at any time broader than for the Lu-based glass. The cyclic heat treatment of the samples allowed to directly measure on growing grains the growth ratio presented in Fig. 8, which is defined as $\Delta l/\Delta d$ and describes growth in length for a given growth in diameter in a short time δt. Grain growth can be derived for any starting grain morphology (defined as a data couple aspect ratio–diameter) using the following algorithm.

Growth ratio GR is defined as

$$\mathrm{GR} = \frac{\Delta l}{\Delta d} \tag{2}$$

with Δl the length increase and Δd the diameter increase during the same dwell-time, so that the aspect ratio AR_t at any time t is described by

$$\mathrm{AR}_t = \frac{L_0 + \Delta l_t}{D_0 + \Delta d_t} = \frac{L_0 + \mathrm{GR} \times \Delta d_t}{D_0 + \Delta d_t} \tag{3}$$

with L_0 and D_0 as the length and diameter measured on any grain after either melting or 2 or 8 h dwell-time at 1600 °C. The evolution of the aspect ratio of any grain can be thus calculated from Eq. (3) as its diameter increases, reflecting in this way some state at a higher

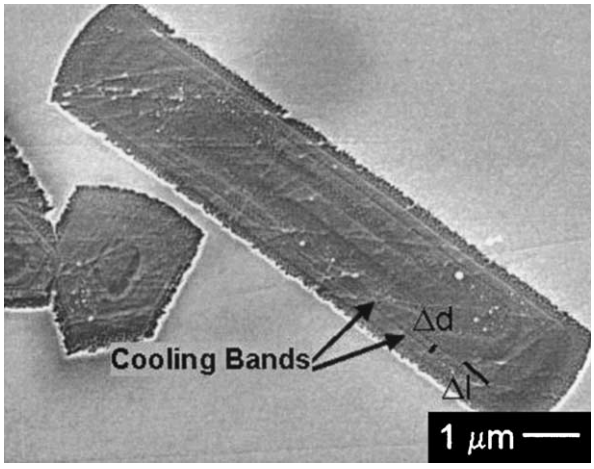

Fig. 7. Plasma etched silicon nitride grain with transient growth bands, in the Y–Si–Mg–O–N glass. Δd and Δl mark the net growth during one heat-treatment.

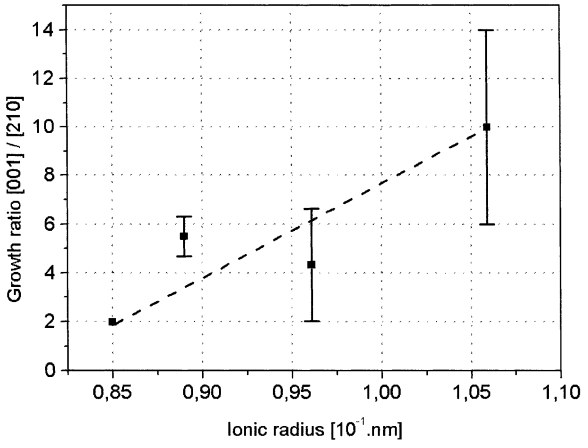

Fig. 8. Growth ratio as a function of the Me^{3+} radius.

dwell-time, for example the 18 h state measured in this experiment. As an example, the growth of 3 grains with either high aspect ratio and low diameter, high diameter and low aspect ratio or mean aspect ratio and diameter is showed in Fig. 9. Grains with higher aspect ratios as the growth ratio will grow with a decreasing aspect ratio. Grains with a lower aspect ratio as the growth ratio will grow with an increasing aspect ratio, so that the morphology of any growing grain tends to be the same and depends neither on the starting aspect ratio nor on the starting diameter.

The current aspect ratio and diameter of a grain only influences the kinetics with which the grain will reach the convergence value of the aspect ratio. With decreasing grain diameter, the convergence value of the aspect ratio is achieved faster. The near equilibrium aspect ratio derived from the largest grains of a distribution coincides with the convergence value calculated from the growth ratio. Thereafter it is only determined by the growth ratio, i.e. the anisotropy of growth. From this representation, it becomes also clear that grain growth anisotropy is only determined by the growth ratio, which changes with the composition of the surrounding glass (Fig. 8). It seems thus quite doubtful, that the aspect ratio of the largest grains of a distribution would increase again after having reached the convergence value, as suggested in Ref. 15. This could only be the result of an increase of the growth ratio, due to changes in supersaturation of the glass matrix.

4.2. Growth anisotropy and glass composition

Grain growth mechanism of silicon nitride has been shown to depend primarily on the atomistic character of the prism [crystallographic (100)] and basal [crystallographic (001)] planes of β-grains.[19] The basal planes are atomically rough, so that grain growth in the crystallographic [001] direction is diffusion controlled. Growth in the crystallographic [210] direction occurs via 2D-nucleation, and is therefore attachment controlled. Growth rates of both basal V_B and prism V_p planes, as a function of the driving force for grain growth, are thereafter described by the Eqs. (4) and (5), as established by Hartman,[32]

$$v_B = K \cdot S_c \tag{4}$$

$$v_P = K_1 \cdot \ln(S_c)^{1/6} \cdot \exp\left[-\frac{K_2}{\ln S_c}\right] \tag{5}$$

where S_c is the supersaturation, which in our case where temperature is constant corresponds to the driving force, K_1 and K_2 are two constants that describe the kinetics of the attachment reaction on the prism planes. The increase of V_B and V_P as a function of S_c is plotted in Fig. 10 for arbitrary values of K_1 and K_2. The growth rate of the basal plane is diffusion controlled and therefore linearly dependent on supersaturation. Anisotropy of growth, i.e. the ratio V_B/V_P, correlates directly with the growth ratio measured in grains.

We assume supersaturation to be constant during the complete annealing. Indeed, at each time, the smallest β-grains of the distribution dissolve because their equilibrium concentration is lower than the mean concentration in the surrounding glass. By doing so, a constant supersaturation is always assured in the glass. Furthermore, if a mechanism of attachment controlled growth is assumed for the prism planes then, at any time, diffusion is not the rate limiting step, so that no composition gradient appears and the supersaturation around each grain is constant. Supersaturation, which is here equivalent to nitrogen oversaturation of the glassy matrix, is nearly constant in all glass compositions. The six compositions contain 1 eq-% N more than the

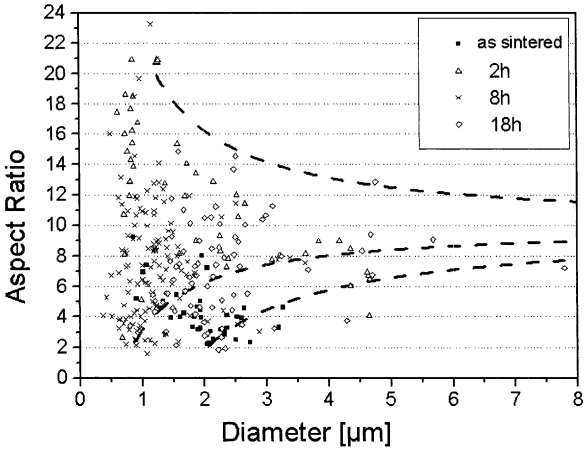

Fig. 9. Distribution of the aspect ratios as a function of the diameter of the particles depending on dwell-time at 1600 °C for the La-based glass. Dotted-lines represent the calculated evolution of the aspect ratio when the diameter increases, according to the growth ratio in Fig. 8.

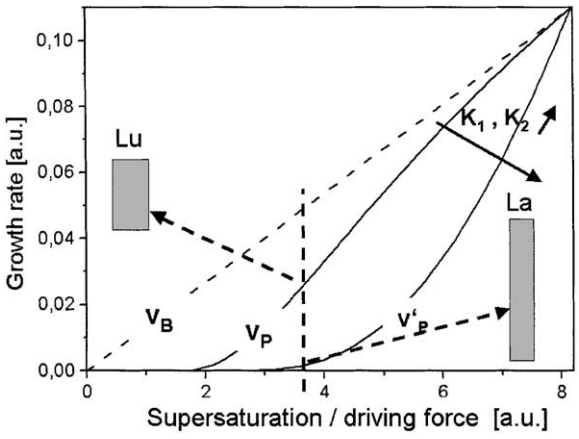

Fig. 10. Graphical representation of growth velocities of the prism and basal planes as a function of the supersaturation and deducted near-equilibrium aspect ratio.

solubility limit of each glass, which is a function of the Me^{3+} cation and was determined at 1700 °C as reported elsewhere).[33] For the v_B and v_P curves in Fig. 10, at an arbitrary supersaturation, the growth ratio and near-equilibrium aspect ratio match the value measured in the glass with small Me^{3+} cations, for example the Lu-based glass. Since supersaturation is constant in all glass samples and $v_B = f(S_c)$ is the same for all compositions, a variation of the growth ratio and the near equilibrium aspect ratio can only be a consequence of a variation of v_P. An increase of K_1 and K_2, that implies lower kinetics of the attachment on the (100) planes, corresponds to a new v'_p curve, for which the ratio V_B/V_P increases. The new growth ratio and corresponding expected near-equilibrium aspect ratio coincides with the values measured in the glasses with large Me^{3+} cations like La^{3+}.

The surface energy and resulting equilibrium shape of β silicon nitride as described by Kraemer for grains in vacuum, do not explain the variation of growth anisotropy from 2 to 10 with the composition of the glass. It is though, a condition for anisotropic growth as attachment on the (001) planes is always energetically favored compared to the attachment on the (100) planes. The difference in growth anisotropy with the composition of the glass suggests that interfacial properties significantly change with the radius of the Me^{3+} cation. In the Lu-based glass growth anisotropy is very low. It nearly corresponds to the theoretical grain form calculated from the ratio of the attachment energies for grains in vacuum.[19] Therefore one can assume that the Lu-ion does not greatly influence the theoretical attachment mechanism on the (100) planes. If the glass contains large Me^{3+} ions, the attachment kinetic on the prism planes decreases and as a consequence growth anisotropy increases. According to this model, the differences in grain growth anisotropy are solely caused by the change in the kinetic of the attachment controlled reaction at the (100) planes, for which Me^{3+} radius is a key issue.

Kanamaru made the assumption, in Si–Al–RE–O–N glasses, that grain growth mechanism of the prism planes changes from diffusion (for RE = Yb) to attachment (for RE = La) controlled with increasing size of the RE cation. In the present experiment, the prism planes of β-grains, independently of the Me^{3+} radius, remained flat (Figs. 11 and 12). This indicates an attachment controlled growth for all glass composition, and justifies the assumption above, for the expression of growth velocity of the prism planes [Eq. (5)]. The transient growth bands that form during cooling and reheating and are revealed by the etching process, are deeper etched when the Me^{3+} radius increases (Figs. 11 and 12). The etching process is accelerated when impurity content increases. Me^{3+} cations can be impurities but are not soluble in the Si_3N_4 crystal under thermodynamical equilibrium conditions. Therefore, one can assume an absorbed layer of Me^{3+} ions at the grain/glass interface. Because of the high supersaturation during cooling, growth velocity of the grain could be higher than diffusion of the Me^{3+} ions, so that those would stay trapped in the Si_3N_4 lattice after cooling. A higher etching of the transient growth bands indicates thus a higher absorption of Me^{3+} ions at the interface. As a conclusion, it seems, that with increasing radius, Me^{3+} cations adsorb more readily at the interface, what hinders the attachment of growing units on the (100) planes. As a consequence, reaction constants K_1 and K_2 in Eq. (5) as well as anisotropy of growth increase.

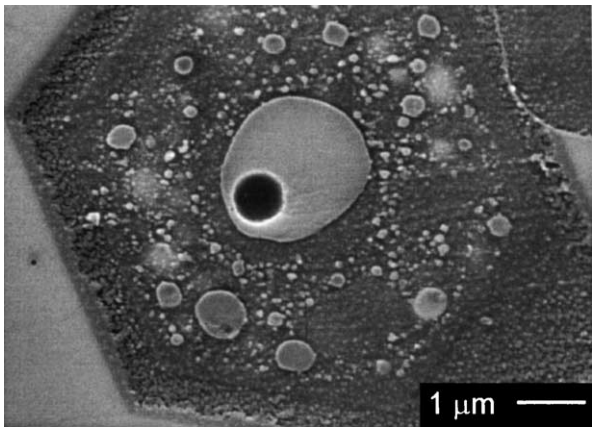

Fig. 11. SEM micrograph of the basal section of a growing β-Si_3N_4 grain in the Lu-based glass.

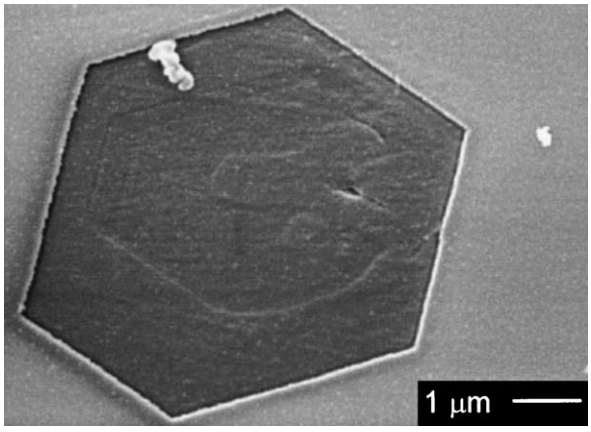

Fig. 12. SEM micrograph of the basal section of a growing β-Si_3N_4 grain in the La-based glass.

5. Conclusions

Systematic investigations of the Ostwald ripening behavior of β-silicon nitride grains dispersed in Me–Mg–Si–O–N glasses have brought some insights on the impact of Me^{3+} cations (Me = La, Lu, Sc, Sm, Y, Yb) on grain growth anisotropy of silicon nitride.

Typical aspect ratio–diameter distributions at the end of the α-β transformation, known from the literature, were confirmed for all compositions. Only the range of the aspect ratio is a function of Me^{3+} radius. Flattening of the distribution during anisotropic Ostwald ripening was observed for all compositions. We showed that the kinetics were greatly influenced by the starting size of the grains, but that all grains grow to a converging value, which has been defined as near-equilibrium aspect ratio.

The growth ratio, measurable directly on the grains that underwent cyclic heat treatment, predicts as equilibrium form the same value as expected from Ostwald ripening analysis. We therefore conclude that grain growth anisotropy is solely determined by the Me^{3+} cation size.

The increase in anisotropy of growth observed with increasing radius of Me^{3+} is explained by increasing reaction constants for the attachment reaction on the prism planes. Lower attachment kinetics for larger Me^{3+} cations is a consequence of a favored adsorption of Me^{3+} onto the (100) planes when cation size increases, what was revealed by plasma etching experiments.

Acknowledgements

Financial support from the European Community "Growth"-Programm, NANOAM project contract Nr.GRD2-200-3030351, is gratefully acknowledged.

References

1. Lange, F., Relation between strength, fracture energy, and microstructure of hot-pressed Si_3N_4. *J. Am. Ceram. Soc.*, 1973, **56**(10), 518–522.
2. Himsolt, G., Knoch, H., Huebner, H. and Kleinlein, F., Mechanical properties of hot-pressed silicon nitride with different grain structures. *J. Am. Ceram. Soc.*, 1979, **62**(1–2), 29–32.
3. Kawashima, T., Okamoto, H., Yamamoto, H. and Kitamura, A., Grain size dependence of the fracture toughness of silicon nitride ceramics. *J. Ceram. Soc.*, 1991, **99**(4), 320–323.
4. Hoffmann, M., Analysis of microstructure development and mechanical properties of Si_3N_4. In *Tailoring of Mechanical Properties of Si_3N_4 Ceramics*, ed. M. Hoffmann and G. Petzow. Kluwer Academic Publishers, Netherlands, 1994, pp. 59–72.
5. Hirao, K., Nagaoka, T., Brito, M. and Kanzaki, S., Microstructure control of silicon nitride by seeding with rodlike β-silicon nitride particles. *J. Am. Ceram. Soc.*, 1994, **77**(7), 1857–1862.
6. Mitomo, M., In-situ microstructural control in engineering ceramics. *Key Eng. Mat.*, 1999, **161–163**, 53–58.
7. Peillon, F. C. and Thevenot, F., Microstructural designing of silicon nitride related to toughness. *J. Eur. Ceram. Soc.*, 2002, **22**, 271–278.
8. Sanders, W. and Mieskowski, D., Strength and microstructure of sintered Si_3N_4 with rare-earth-oxide additions. *Am. Ceram. Soc. Bull.*, 1985, **64**(2), 304–309.
9. Goto, Y. and Thomas, G., Microstructure of silicon nitride ceramics sintered with rare-earth oxides. *Acta Metall. Mater.*, 1995, **43**(3), 923–930.
10. Pyzik, A. and Beaman, D., Microstructure and properties of self-reinforced silicon nitride. *J. Am. Ceram. Soc.*, 1993, **76**(11), 2737–2744.
11. Kitayama, M., Hirao, K., Toriyama, M. and Kanzaki, S., Control of β-Si_3N_4 crystal morphology and its mechanism (part 2)—effect of lanthanide additives. *J. Ceram. Soc. Jap.*, 1999, **107**(11), 995–1000.
12. Lifshitz, L. and Slyozov, V., The kinetics of precipitation from supersaturated solid solutions. *J. Phys. Solids*, 1961, **19**(1–2), 35–50.
13. Wagner, C., Theorie der alterung von niederschlaegen durch umloesen (ostwald reifung). *Zeitschrift fuer Elektrochemie*, 1961, **65**, 581–591.
14. Bernard-Graner, G., Yeckley, R. and L'Amoulen, R., Densification and grain growth kinetic for silicon nitride. *Key Eng. Mat.*, 1997, **132–136**, 892–895.
15. Kitayama, M., Hirao, K., Toriyama, M. and Kanzaki, S., Experimental evidence for the anisotropic ostwald ripening of β-silicon nitride. *J. Am. Ceram. Soc.*, 1999, **82**(10), 2931–2933.
16. Kitayama, M., Hirao, K., Toriyama, M. and Kanzaki, S., Modeling and simulation of grain growth in Si_3N_4—i. Anisotropic ostwald ripening. *Acta Mater.*, 1998, **46**(18), 6541–6550.
17. Kraemer, M., Hoffmann, M. and Petzow, G., Grain growth of silicon nitride dispersed in an oxynitride glass. *J. Am. Ceram. Soc.*, 1994, **76**(11), 2778–2784.
18. Dressler, W., Kleebe, H., Hoffmann, M., Ruehle, M. and Petzow, G., Model experiments concerning abnormal grain growth in silicon nitride. *J. Eur. Ceram. Soc.*, 1996, **16**, 3–14.
19. Kraemer, M., Wittmuess, D., Kueppers, H., Hoffmann, M. and Petzow, G., Relations between crystal structure and growth morphology of β-Si_3N_4. *J. Cryst. Growth*, 1994, **140**, 157–166.
20. Hampshire, S. and Jack, K., The kinetics of densification and phase transformation of nitrogen ceramics. In *Special Ceramics. 7. Proc. Brit. Ceram. Soc., Hrsg*, ed. D. Taylor and P. Popper, 1981, pp. 37–49.
21. Hirosaki, N., Okada, A. and Matoba, K., Sintering of si_3n_4 with the addition of rare-earth oxides. *J. Am. Ceram. Soc.*, 1988, **71**(3), C–144-C-147.
22. van Weeren, R. and Danforth, S., The effect of grain boundary phase characteristics on the crack deflection behavior in a silicon nitride material. *Scripta Mat.*, 1996, **34**(10), 1567–1573.
23. Wang, C.-M., Pan, X., Hoffmann, M., Cannon, R. and Ruehle, M., Grain boundary films in rare-earth-glass-based silicon nitride. *J. Am. Ceram. Soc.*, 1996, **79**(3), 788–792.
24. Becher, P., Waters, S., Westmoreland, C., Riester, L. Compositional effects on the properties of Si–Al–Re based oxynitride glasses. *J. Am. Ceram. Soc.*
25. Menke, Y., Peltier-Baron, V. and Hampshire, S., Effect of rare-earth cations on properties of sialon glasses. *J. Non-Cryst. Solids*, 2000, **276**, 145–150.
26. Kanamaru, M., *Untersuchung zur gefuegeentwicklung von si_3n_4-keramiken mit seltenen erdoxiden*. PhD thesis, Institutue Metalikunde der Universitaet Stuttgart und Max-Planck-Institut fuer Metallforschung, Institut flier Werkstoffwissenschaft 1994.
27. Murakami, Y. and Yamamoto, H., Properties of oxynitride glasses in the Ln–Si–Al–O–N systems (Ln = rare-earth. *J. Ceram. Soc. Jap.*, 1994, **102**(3), 231–236.
28. Petzow, G., *Metallographisches, keramographisches, plastographisches Aetzen, 6. ueberarbeitete Version (Materialkundlich-Technische Reihe; 1)*. Gebrueder Borntraeger, Berlin Stuttgart, 1994.
29. Wang, C.-M., Pan, X., Gu, H., Duscher, G., Hoffmann, M., Cannon, R. and Ruehle, M., Transient growth bands in silicon nitride cooled in rare-earth-based glass. *J. Am. Ceram. Soc.*, 1997, **80**(6), 1397–1404.
30. Kraemer, M., Hoffmann, M. and Petzow, G., Grain growth kinetics of β-Si_3N_4 during α/β-transformation. *Acta Metall. Mater.*, 1993, **41**(10), 2939–2947.

31. Kraemer, M., Untersuchung zur wachstuinskinetik von β-Si_3N_4 in keramiken und oxinitridglaesern. PhD thesis, Institut fuer Metalikunde der Universitaet Stuttgart und Max Planck Institut fuer Metallforschung, Institut flier Werkstoffwissenschaft, 1991.
32. Hartman, P., Modern pbc theory. In *Morphology of Crystals, Part A, B, Terra-Scientific Publishing Comp. (TERRAPUB)*, ed. I. Sunagawa. , 1987, pp. 269—319.
33. Satet, R., Holzer, S., and Hoffmann, M. Crystalline phases and nitrogen solubility limit of Me–Si–Mg–O–N glasses with Me = La, Lu, Sc, Sm, Y and Yb compared to Me–Si–Al–E–N glasses with Me La, Gd, Nd and Yb. (to be published).
34. Shannon, R. and Prewitt, C., Effective ionic radii in oxides and fluorides. *Acta Cryst. B*, 1969, **25**, 925–946.